J Nanostruct 12(2): 287-302, Spring 2022

RESEARCH PAPER

Preparation of Multi-purpose Nano Ink-jet Printed Fabric by Pretreating Cotton Fabric with Carboxylated Styrene-Butadiene Latex

Ali Goudarzi [1], *Atasheh Soleimani-Gorgani* [1]*, *and Ozan Avinc* [2]

[1] *Department of Printing Science and Technology, Institute for Color Science and Technology, Tehran, Iran*

[2] *Department of Textile Engineering, Engineering Faculty, Pamukkale University, Denizli, Turkey*

ARTICLE INFO

Article History:
Received 18 November 2021
Accepted 18 March 2022
Published 01 April 2022

Keywords:
Carboxylated styrene-butadiene latex
Conductive
Cotton fabric
E-textile
Inkjet printing
Silver nanoparticles

ABSTRACT

Flexible electronic printing devices have drawn significant attention due to the economic approach. Cotton fabric's porosity and high surface roughness avoid electrically conductive printed patterns on the fabrics. In this study, the cotton fabric was pretreated with carboxylated styrene-butadiene latex (XSBL) with the pad-dry-cure process for in situ solution deposition of silver free particles inkjet ink. The pretreating process did not have an adverse effect on thermal behavior and colorimetric properties and improved the fabric's crease recovery angle and hydrophobicity. The pretreated and untreated fabrics were printed through the HP Deskjet inkjet printer with one, five, and ten printing layers of formulated water-based silver free-particles ink for comparison. XRD analysis illustrated the crystal structure of silver nanoparticles on the printed pretreated cotton fabric. FE-SEM and EDS analysis indicated that the presence of silver nanoparticles increased by increasing the number of printing runs. Repetition printing sequences increased average particle size, growing grain size (52 nm to 90 nm). It was determined that the presence of XSBL on the fabric surface provides a suitable structure, with resistance (25 ohms) and antibacterial activity against gram-positive and gram-negative bacteria for use in multi-purpose inkjet printing cotton fabric. The printed pretreated fabrics exhibited appropriate washing fastness properties due to the cross-linked structure between free carboxylic groups of XSBL resin and hydroxyl groups of cellulose. It is the first time using an economical polymer layer on cotton fabrics to provide robust, flexible electronic inkjet printed fabric with great potential for commercial mass production.

How to cite this article
Goudarzi A, Soleimani-Gorgani A, Avinc O. Preparation of Multi-purpose Nano Ink-jet Printed Fabric by Pretreating Cotton Fabric with Carboxylated Styrene-Butadiene Latex. J Nanostruct, 2022; 12(2):287-302. DOI: 10.22052/JNS.2022.02.007

INTRODUCTION

Printed electronic textiles have drawn attention in recent years. To meet today's market's needs, providing customer's ideal design, cost-effective and environmentally-friendly inkjet printers were introduced to the industry [1-3]. In the past, mostly the lithography method and dip-coating methods were considered. In the lithography method, there are some steps, such as etching and plating, which are time-consuming and costly. The dip-coating method suffers from a time-consuming production process, small mass loadings, inability

* *Corresponding Author Email: asoleimani@icrc.ac.ir*

to create patterns, relatively loosely bonding, and uneven distribution. The traditional printing methods such as gravure [4, 5], flexography [6, 7], and screen printing [8, 9] are also used to deposit the conductive inks; due to their limitations, the efforts are put into using inkjet printing method [10, 11]. In addition, the inkjet printing method is capable of easy application and flexibility in pattern changing and the ability of printing on a large scale, which makes it an appropriate alternative for traditional printing methods [12, 13]. The conductive patterns printed by inkjet printers have gained more attention than other processes due to their simplicity and cost-effectiveness. As a digital printing method, inkjet printing has many other advantages such as low cost, low contamination, low materials waste, and high precision compared to traditional printing methods [2, 14]. Conductive inks as the newest ink generation are applicable in many different applications such as organic light-emitting diodes (OLEDs) [11, 12], radio-frequency identifications (RFIDs) [15, 16], solar cells [10], flexible electronics [17, 18], antennas [19], sensors and electric circuits [13, 20]. Different methods are used to apply conductive ink on the substrate. In previous studies, conductive fabrics based on the cotton were prepared using various methods such as coating [21], knife over rolls [22], spraying [23]¥ ⍰%0-, and dip-coating [24] by applying conductive nano metals on the fabric. These methods were based on the surface coverage and not a specific desired pattern. From conductive inks to fabricating printed circuits, silver nanoparticles have unique applications. Several methods for producing silver nanoparticles are divided into physical, chemical and photochemical approaches (25) and, recently, bio methods [25-27]. The chemical reduction approach is more predominant due to the ease of process and decrement of costs [28]. A conductive layer based on silver nanoparticles with a redox reaction on the various substrates was examined in previous studies [14, 29]. In recent years, using silver complex-based inks due to their advantages has been hugely considered [30, 31]. The free-particle silver complex inkjet ink is a single-stage process without nozzle clogging [32, 33]. The physical-chemical properties of prepared inkjet inks are very challenging. Silver complex-based inks with excellent conductivity have advantages such as a single-step process without nozzle clogging due to their free particles [30].

Cotton is one of the most consumed fibers in the world. The elasticity of the dry and wet cotton fibers is generally low, so many finishing processes are done on the cotton to improve crease-resistance [34]. The hydroxyl groups on cotton's chemical structure provide an excellent affinity for the fabric. Despite cotton's softness and high moisture absorption, some pretreatment must be carried out due to cotton's high creasing and penetrating [35]. In high heat treatment temperature, yellowing and cotton degradation temperature should also be considered.

Carboxylated styrene-butadiene latex (XSBL) is a copolymer of styrene and butadiene with enhanced properties compared to the non-carboxylated one and is also available in water-based emulsion form [36]. This milky emulsion consists of repeated styrene/butadiene units and carboxylic functional groups attached to the main chain. Mostly styrene units are responsible for polymer toughness, while butadiene units mainly control the impact ability of the final polymer. In non-carboxylated styrene-butadiene resins, the formed film had many advantages like abrasion resistance, low cost, transparency. However, its chemical resistance and mechanical properties must be improved [37, 38]. Introducing the carboxylic group to the polymer's main chain provides a suitable cross-linked structure with the appropriate chemical resistance [39]. XSBL resin has numerous applications in different industry such as the textile and paper industry. Using XSBL in finishing textiles and carpets improves the mechanical properties and increases its pigment ability [36].

In the current work, due to the chemical and physical advantages of XSBL, it was selected for the pretreatment process of the cotton fabric for the first time to resist ink penetration into the fabric and improve conductivity. The cotton fabrics were treated with XSBL solution and printed with water-soluble silver free particles ink. The pretreatment process also improved the wash fastness of the printed silver nanoparticles. The obtained results confirm that the flexible electronic printed fabric can be used as a multifunctional electronic textile with great potential for commercial mass production.

MATERIALS AND METHODS

Carboxylated styrene-butadiene latex (XSBL) resin (Tg= -15) was purchased from resin polymer

(Iran). Silver acetate and formic acid were purchased from Merck Company (Germany). Woven fabric used was 100% singed, desized, scoured, and bleached cotton plain weave fabric (98 g/m^2) supplied by the Broojerd Textile Company (Iran). All the reagents were analytical grade.

Pretreatment of the cotton fabrics XSBL solutions

The pretreatment of the cotton fabrics was performed by padding process using a padding machine (Ernst Benz, Germany) with a pressure of 5 kg/cm^3 and at a constant padding speed of 3.5 m/min with the 80% wet pick-up. The pretreated cotton fabric was dried in an Azar 1250 furnace (AzarFurance Company, Iran) at 120˚C for 3 minutes. The reflectance spectra of the pretreated and untreated cotton fabrics were obtained in the wavelength range of 400 nm to 700 nm using a GretagMacbeth Spectrophotometer Color-Eye7000A (Xrite Company, New York, USA). Thermal behaviors of the pretreated and untreated cotton fabrics were analyzed using Thermo Gravimetry/Differential Thermal Analyzer (Perkin Elmer, Pyris Diamond SII, USA) in an air atmosphere at a heating rate of 10 ˚C /min. The contact angles were measured by a device (OCA20, Data Physics, Germany) equipped with GAOSUO software-operated camera to capture the drop images. The tensile strength (tensile stress) and elongation (tensile strain) values of untreated and pretreated cotton fabrics were investigated by Instron (5566, USA) instrument, according to the ASTM D5035 standard. The crease recovery angle values were assessed using a crease recovery tester (DAIEI KAGAKU SEIKI MR-1) according to the ISO 2313 standard. Fourier transformed infrared spectroscopy in attenuated total reflection mode (ATR-FTIR) spectrums on Nicolet (Nexus 670, USA) in the range 400–4000 cm^{-1} were examined to characterize untreated and pretreated cotton fabrics. Yellowness (Whiteness) is associated with scorching, soiling, and product degradation by exposure to light or chemicals. Thus, the yellowness index, ASTM E313 defines, can indicate color degradation after treatment by comparing the treated and untreated specimens. pH value of treated and untreated fabrics determined by ISO 3071 standard.

Ink preparation

First, silver acetate (1g, 0.00599 mol) was added to ammonium hydroxide (2.5g,0.0071 mol) while vortex mixing at ambient temperature for 15 seconds. Afterward, formic acid was added to the solution dropwise for 60 seconds. The solution color turned dark grey, showing silver ions' reduction to silver particles. After 12 hours, a clear solution was obtained by the precipitation of large particles. The clear solution was filtered using a syringe filter (200 nm). The obtained solution containing 22%wt silver was used as a silver complex and the ink base in the following steps.

Printing process

Treated cotton fabrics glued to papers to be suited for printing propose. Afterward, the black cartridge of the HP printer was removed. The cartridge has been washed and then filled with prepared ink. After cartridge placement, the printing process starts, set to use only black cartridge on maximum dpi mode. After printing, the cotton fabrics were subsequently dried at 120 ˚C for 5 minutes using Azar 1250 furnace (Iran) to produce and fix silver nanoparticles. Then the printed cotton fabrics were washed with distilled water to remove any contamination or unreacted reagents from the fabrics. A four-point probe instrument (Soraco, Iran) was used to measure the surface resistance of printed cotton fabrics. Furthermore, the ampere/voltage diagrams and conductivity of printed films were assessed using a Keithley (2602, USA) instrument at ambient temperature.

Field emission scanning electron microscope (FE-SEM) instrument (MIRA3, TESCAN, Czech

Table 1. Colorimetric properties of XSBL-pretreated and untreated cotton fabric

Sample	L*	a*	b*	C*	h*	Whiteness Index (CIE)	Yellowness Index (ASTM E313)	ΔE2000
Untreated cotton	90.15	1.45	-3.08	3.4	295.26	91.18	-5.15	-
Pretreated cotton fabric with XSBL	90.00	1.46	-2.27	3.09	298.25	89.19	-4.4	0.33

Republic) determined the surface morphologies of untreated, pretreated, and printed pretreated cotton fabrics. Energy-dispersive X-ray spectroscopy (EDS) using the MIRA3 instrument was also performed for quantitative analysis and the printed cotton fabric's elemental analysis. The crystal structure of printed silver (Ag) nanoparticles was investigated with an X-ray diffractometer (XRD) (GNR, MPD-3000, Italy) instrument at a CuK radiation to evaluate the mineral composition. The wash fastness of printed cotton samples was determined according to AATCC 61-2001 standard test method. The pretreated and printed cotton samples' antibacterial property was carried out using the disc diffusion method ISO 20743.

RESULTS AND DISCUSSION

Effect of pretreating cotton fabric on colorimetric characteristic

Colorimetric values of pretreated and untreated cotton fabrics have been investigated through the L*a*b* system. Color difference, whiteness index, and yellowness index have been calculated and summarized in (Table 1).

The color differences are reported based on two different formulas, but according to ASTM D2244 standard, ΔE2000 is considered for ΔE*<5.

Regarding the white nature of XSBL resin, mainly because of calcium carbonate as an opacifier in the latex, the pretreated cotton fabric did not affect colorimetric values, and color difference was not detectable by human eyes (ΔE<2.4).

Effect of pretreating cotton fabric on thermal behavior

TGA analysis was carried out on untreated and pretreated cotton fabrics. Fig. 1 displays the TGA curves of the samples.

Generally, the decomposition of cotton fibers takes place at three distinct steps. The first step occurs below 100, attributed to the loss of existing moisture trapped inside the fabric, and includes a slight weight loss. The second step, which occurs at ca. 350˚C, is ascribed to the structural decomposition of cellulose accompanied by weight loss of 70%. The third step that gradually happens above 500 is the overall decomposition of the remnant of glucose decomposition [40].

The thermal behavior of samples treated with XSBL depends on the polymerization method, glass transition temperature, and the constituent monomers of XSBL resin [41]. As a thin layer was applied on the cotton fabric surface and the polymer's glass transition temperature was around -15˚C, the relevant changes attributed to XSBL's presence were not detected. The residual

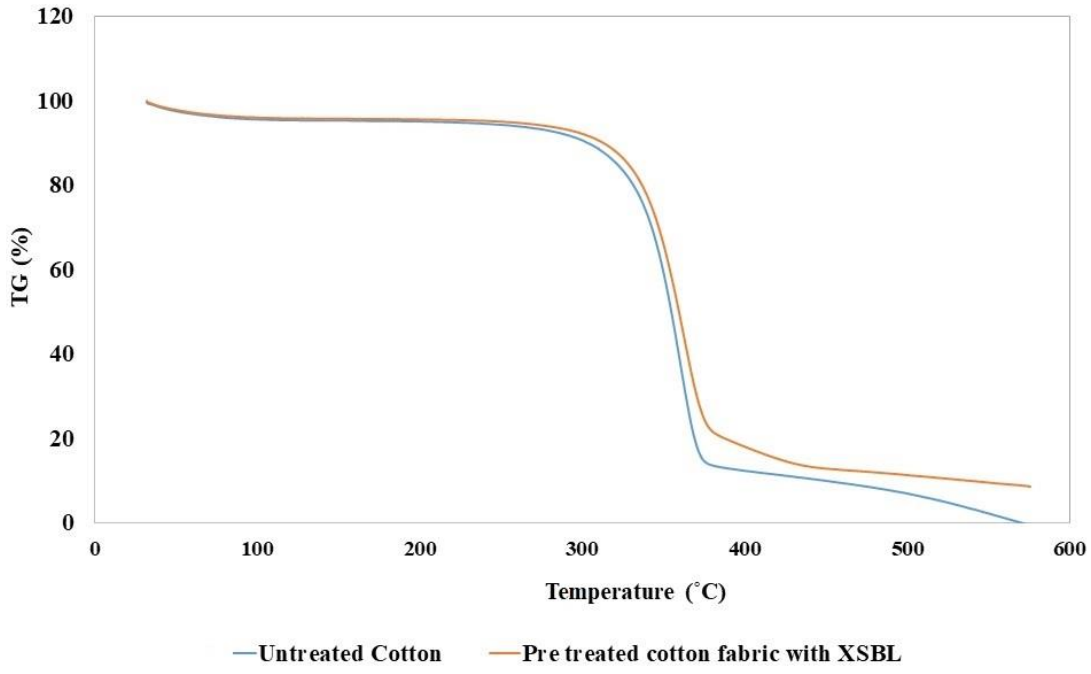

Fig. 1. Thermal behavior of XSBL-pretreated and untreated cotton fabric

of thin resin film had a minor effect on glucose decomposition at above 370˚C. Consequently, pretreating cotton fabric with XSBL resin slightly improves the thermal behavior of the fabric.

Effect of pretreating cotton fabric on the surface energy

One of the methods available for measuring the free surface energy is the angle formed by water on the surface. The following equations can calculate the free surface energy [42-44]:

The work of adhesion (W_A) and energy of the film surface can be calculated from equation 1 (Young's equation) and equation 2 (Newman equation).

$$W_A = \gamma_{LV}(1 + cos\,\theta) \quad (1)$$

$$W_A = 2(\gamma_{LV}\gamma_{SV})^{1/2}\ exp[-\beta(\gamma_{LV} - \gamma_{SV})^2\ ] \quad (2)$$

Where, and are water surface tension, the free energy of the film surface, and the angle formed by water on the film surface, and is the equation constant equal to 0.000124770 $(mj/m^2)^{-2}$. The units of surface free energy are j/m^2 or N/m. The surface tension of water is 72 mj/m^2.

The contact angle of samples with water is shown in Fig. 2, and obtained results are summarized in (Table 2).

According to the obtained results, due to the hydrophobic nature of the polymeric layers formed on the surface, adding a polymeric layer on the cotton fabric increases surface hydrophobicity. The hydrophilic nature declines by applying a layer on the cotton fabric. In addition, the formation of a uniform layer on the surface of cotton fabric leads to decreasing the surface roughness and increasing uniformity. Therefore, the surface energy of cotton fabrics decreased by treating the cotton fabrics with XSBL.

Effect of pretreating cotton fabric on wrinkle recovery angle

Creasability is one of the disadvantages of cotton fabrics. The moisture adsorbed in cotton fibers can simplify the movement of internal polymeric chains, which eliminates the hydrogen bonds available in the cotton structure. Finally, the hydrogen bonds are formed at new sites, which causes the creases [45]. The wrinkle recovery angle value of pretreated and untreated cotton fabric are shown in Fig. 3. After applying XSBL solution and considering the soft hand touching

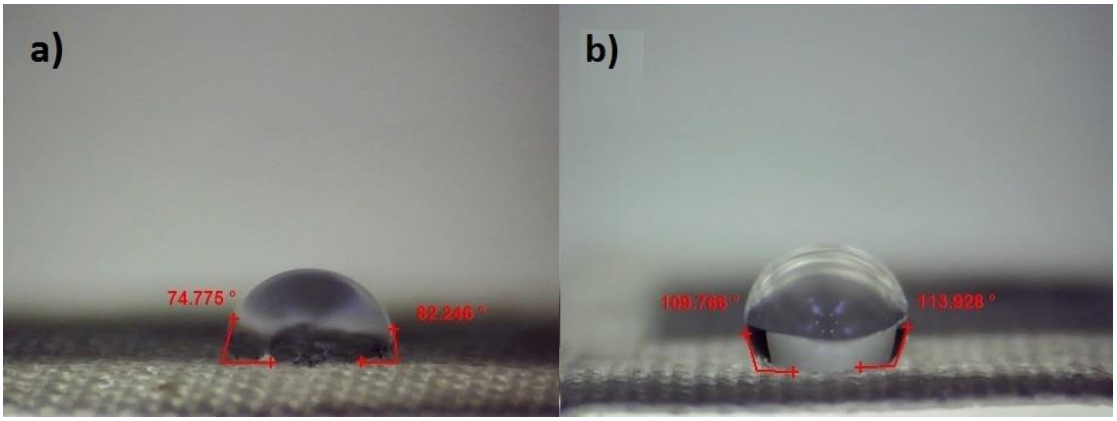

Fig. 2. The contact angle of a) untreated and b) XSBL-pretreated cotton fabric with water

Table 2. The surface energy of XSBL-pretreated and untreated cotton fabric

Sample	Contact angle (°)	Work of adhesion (mj/m^2)	Surface energy (mj/m^2)
Untreated cotton	78	89.96	36.15
Pretreated cotton fabric with XSBL	116	46.19	16.13

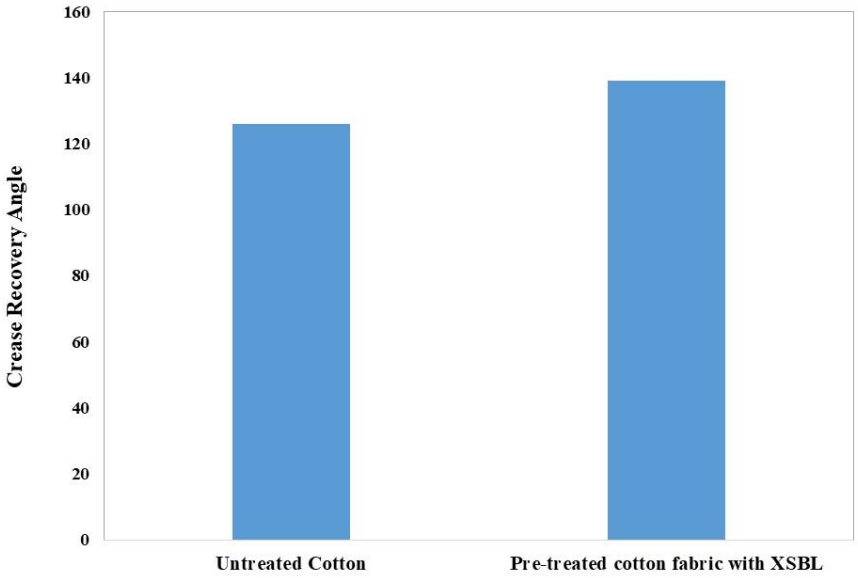

Fig. 3. Crease recovery angle of XSBL-pretreated and untreated cotton fabric

and the carboxylated nature of the XSBL resin, the formation of a new layer on the surface moderately increases crease recovery angle due to limiting the hydrogen bond formation because of the thinly applied polymer layer.

Effect of pretreating cotton fabric on tensile strength and stress value

Fig. 4 represents the stress-strain data of the specimens at the tearing point. It can be concluded that applying an external layer restricted the movement of cellulose chains. Due to the tightening of cellulosic chains, the possibility of chains movement is decreased, so the strain value was less than cotton fabric. The fabric strength was also deteriorated because of applying a polymeric layer.

ATR-FTIR analysis of untreated and pretreated cotton fabric

Fig. 5 represents the ATR-FTIR results of the specimens. In FTIR spectra of untreated cotton

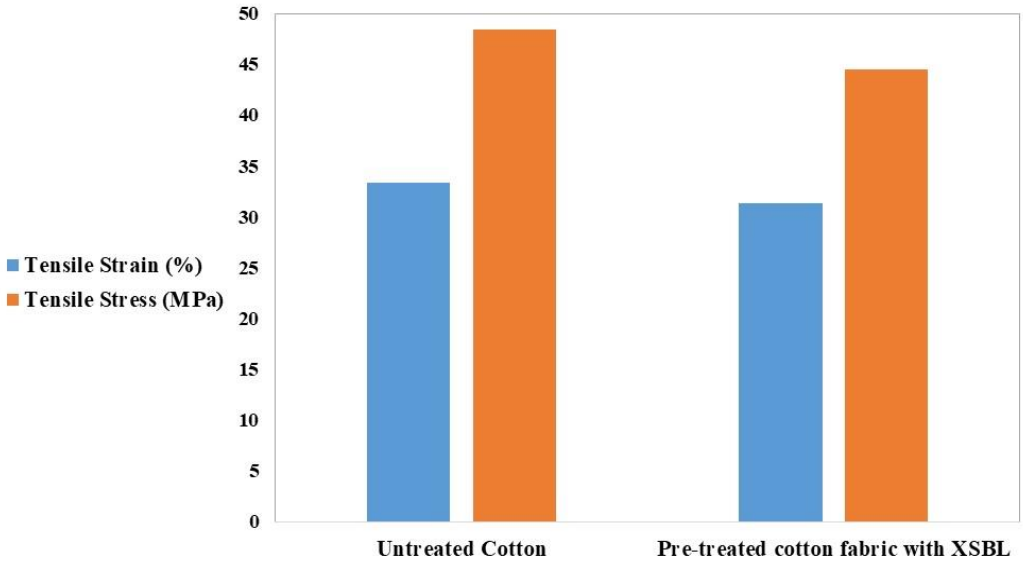

Fig. 4. Tensile strain and tensile stress value of XSBL-pretreated and untreated cotton fabric

fabric, the broad peak at 3263 cm^{-1} is observed, representing the hydroxyl group (-OH) in the cellulose structure of the cotton. The distinct peak at 1730 cm^{-1} is assigned to the stretching of carbonyl (C=O) in untreated cotton due to the factory's sizing and surface modification by formaldehyde and acrylic resin. The peaks at 2872 cm^{-1} and 2915 cm^{-1} are ascribed to the symmetrical and asymmetrical stretching of C-H, and the weak peak at 1312 cm^{-1} is due to the vibrations of hydroxyl groups (-OH). The sharp peak at 1157 cm^{-1} confirms the C-O-C stretching of the cotton structure [46].

The peak that emerged at 1425 cm^{-1} is due to C-H bending, O-C-H, and H-C-H deformation. The peak at 1053 cm^{-1} and 1025 cm^{-1} indicate the C-O, -C-C- and C-C-O groups [47, 48].

In the case of the XSBR specimen, the characteristic peaks of XSBR emerged, which is a sign of surface coverage by XSBL. The signatory peaks appeared at 3330 cm^{-1} (OH stretching), 967 cm^{-1} (1,4 trans butadiene unit), 907 cm^{-1} (1,2 vinyl), 753 cm^{-1} (1,4 cis) and 695 cm^{-1} (styrene unit) [49].

Surface pH of untreated and pretreated fabrics

The pH of the treated sample according to ISO 3071 is presented in (Table 3).

In the case of the untreated sample, as previously mentioned in the ATR-FTIR section, the cotton fabric is prepared using different materials in the sizing and factory finishing process. Acrylate resins and formaldehyde are among these materials responsible for the acidic pH value of untreated cotton fabric. For pretreated cotton fabric with XSBL, the pH decreased due to the carboxylic acid group of the XSBL resin.

FE-SEM analysis of untreated and pretreated fabrics

As seen from the FE-SEM micrographs (Fig. 6), coating an external layer on the cotton covered the surface and affected the porosities. XSBL-pretreated cotton fabric sample had a more uniform surface compared to the untreated cotton fabric sample. The coated layer is thoroughly detectable.

Printing process on untreated and pretreated cotton fabric

Printed patterns on untreated and pretreated cotton fabrics are shown in Fig. 7. Pretreated and untreated fabrics had been printed with one, five, and ten printing layers for comparison.

FE-SEM analysis of printed layers of pretreated

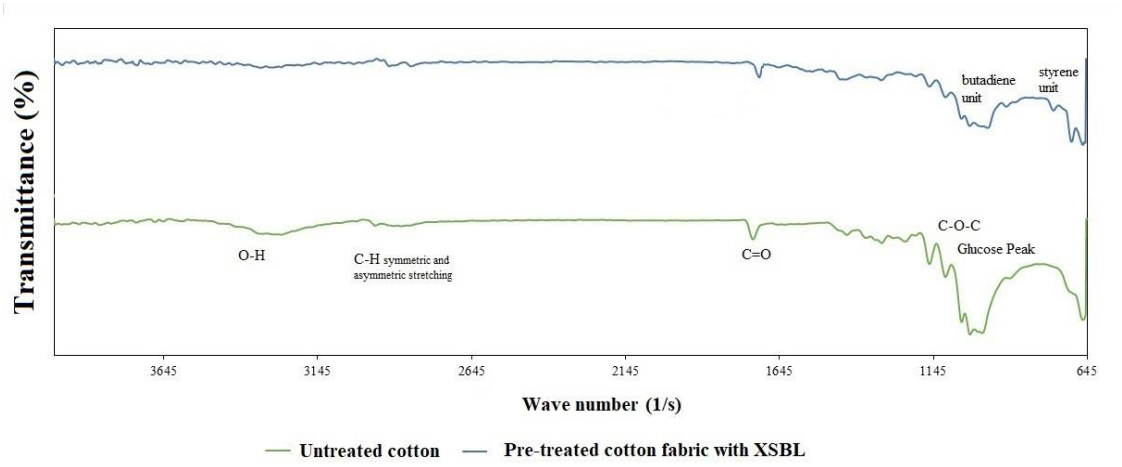

Fig. 5. ATR-FTIR analysis of XSBL-pretreated and untreated cotton fabric

Table 3. pH level value of XSBL-pretreated and untreated cotton fabric

Sample	pH
Pretreated cotton fabric with XSBL	4.64
Untreated Cotton	5.08

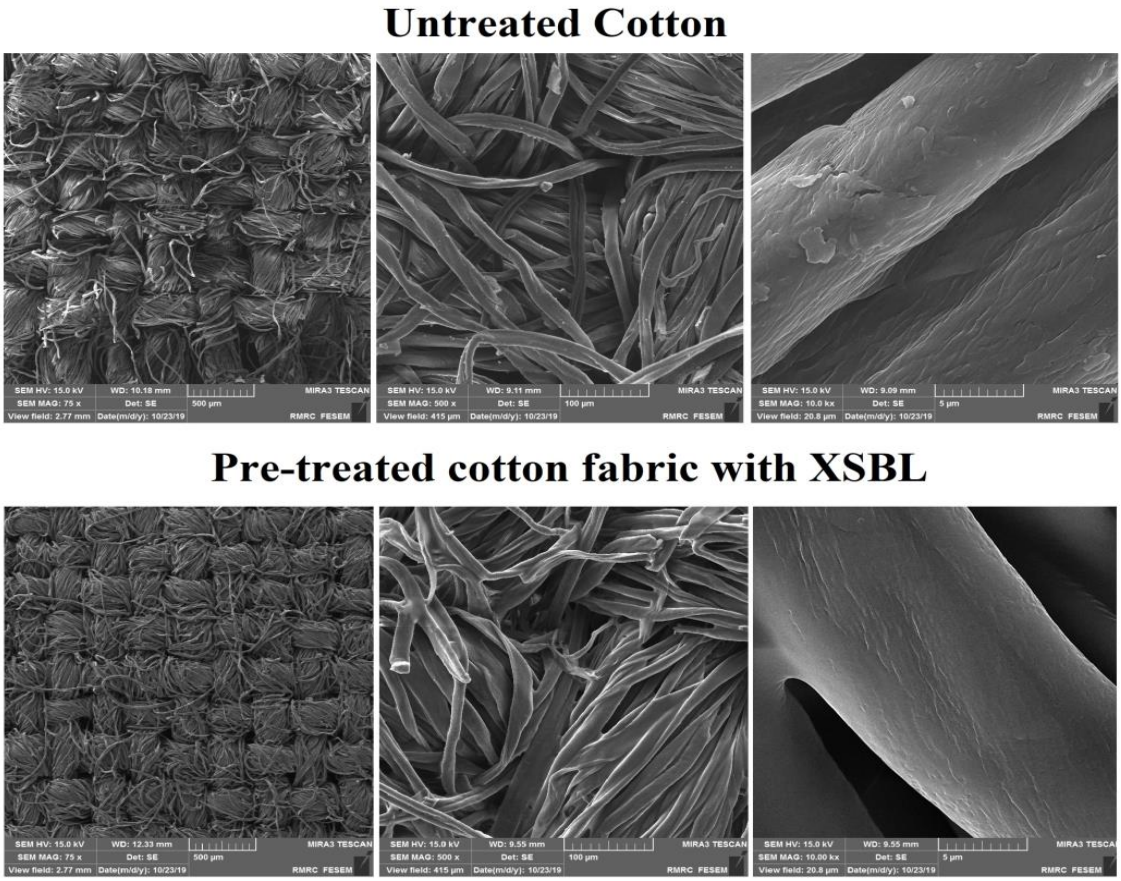

Fig. 6. FE-SEM images of XSBL-pretreated and untreated cotton fabric

cotton fabric with XSBL

Concerning the FE-SEM micrographs in Fig. 8, one layer inkjet printed on the pretreated fabrics diffused into the substrate and did not provide the necessary uniformity. The number of silver nanoparticles on the pretreated cotton fabric surface increased significantly by increasing the printing sequences to five and ten layers.

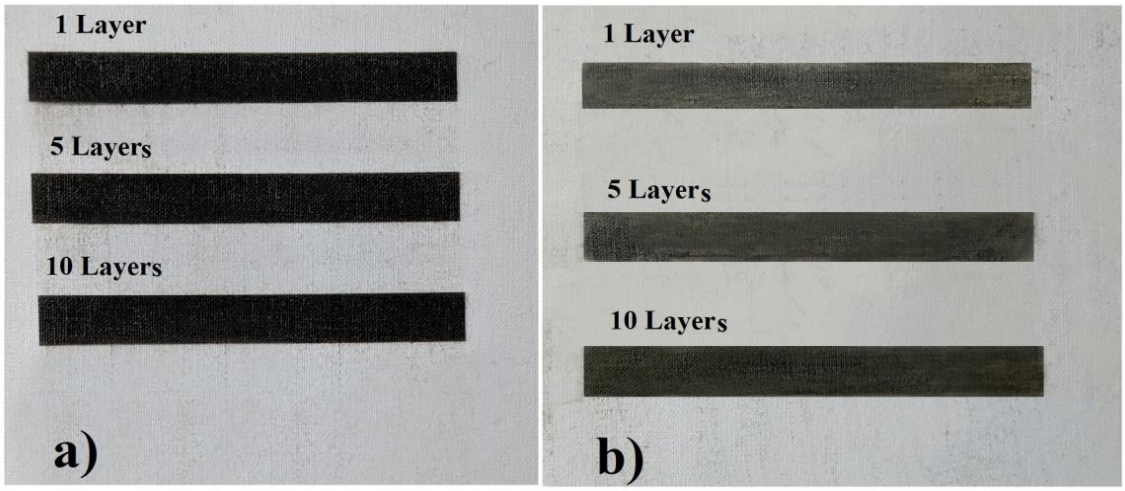

Fig. 7. Image of printed layers on XSBL-pretreated and untreated cotton fabric

Increasing printing sequences caused an increment of nanoparticles concentration on the surface, leading to more surface energy and van der waals attraction, more aggregation of particles, and increased average particle size, resulting in grain size growing (52 nm to 90 nm).

EDS analysis of printed layers

EDS analysis has been conducted to quantify the investigation of printed layers. These results illustrated in Fig. 9 and (Table 4), confirming previous results, indicate that the number of silver nanoparticles on the surface increased by increasing printing runs, which is beneficial to further conductivity measurement.

Conductivity measuring of printed layers

Two different methods were used to measure

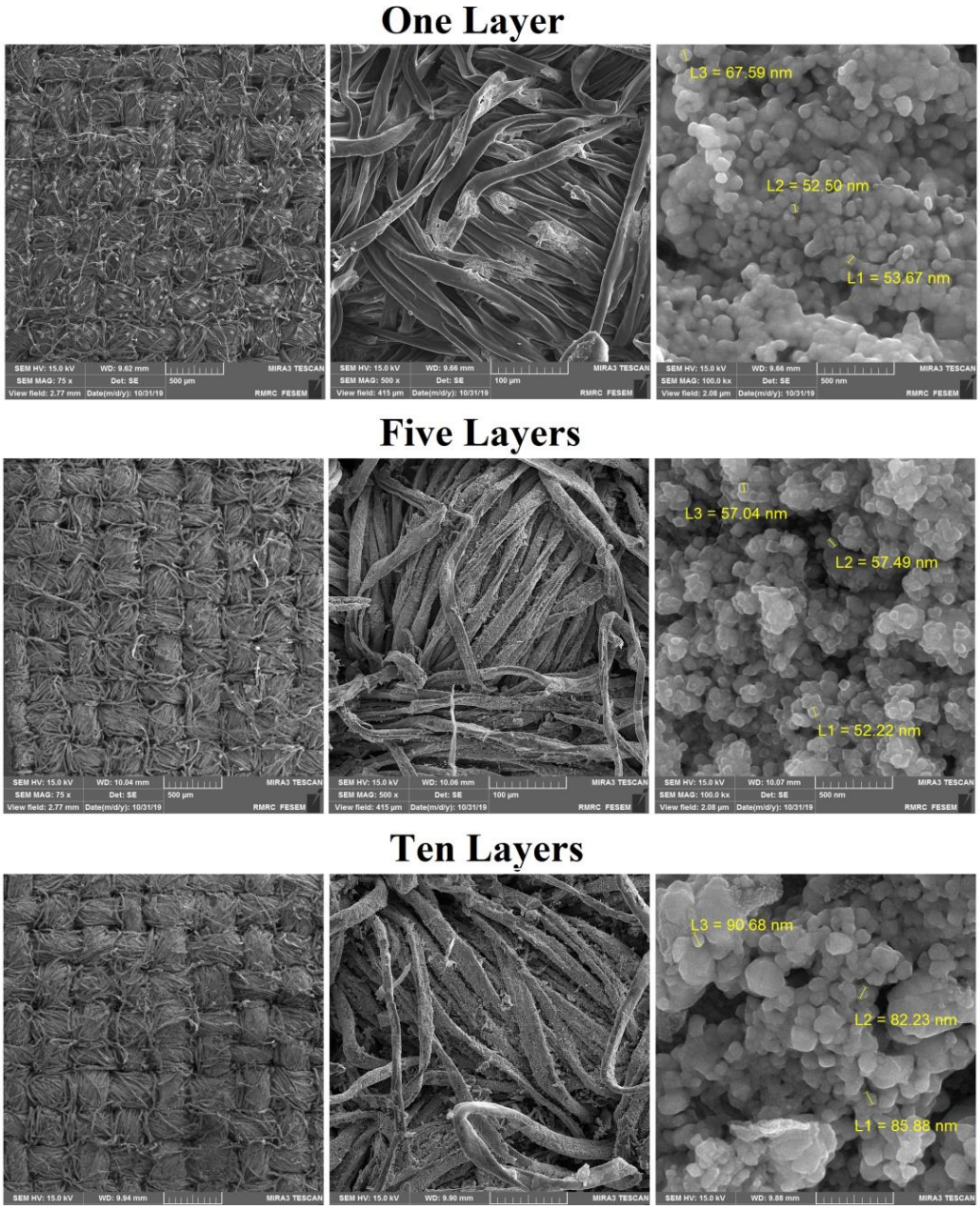

Fig. 8. FE-SEM images of inkjet printed ink on XSBL-pretreated fabric

the printed layers' conductivity/resistivity properties: ampere/voltage diagrams and four-point probe methods. Regarding ampere/voltage diagrams, firstly, a controlled voltage was applied to the specimen, and the electrical current was monitored for the corresponding voltage at every single second, and the results were depicted as a diagram. If the diagram is plotted as ampere/voltage, the slope of the tangent is the criterion of the overall conductivity, which is measured through equation 3 and equation 4. Fig. 10 shows the results of the I-V analysis. The surface resistance of the samples was also measured using four probes instrument, and the result is illustrated in (Table 5).

$$R = \frac{V}{I} \rightarrow \frac{1}{R} = \frac{I}{V} \rightarrow S = \frac{I}{V} \quad (3)$$

$$Slope = \frac{Rise}{Run} = \frac{\Delta y}{\Delta x} = \frac{\Delta I}{\Delta V} = S \quad (4)$$

From the obtained results, it can be concluded that conductivity improved by increasing the printing sequences. For one layer printed sample, conductivity was not detectable. The available silver nanoparticles on the surface were insufficient to form a conductive layer and did not provide the necessary uniformity for electrical conductivity. In addition, a portion of the printed ink was dedicated to diffusion phenomena to the substrate. By increasing the printing sequences, the uniformity improved, diffusion decreased, and conductivity reached an acceptable degree.

One layer of printed specimens had low electrical conductivity, and their resistance was located out of the detection range.

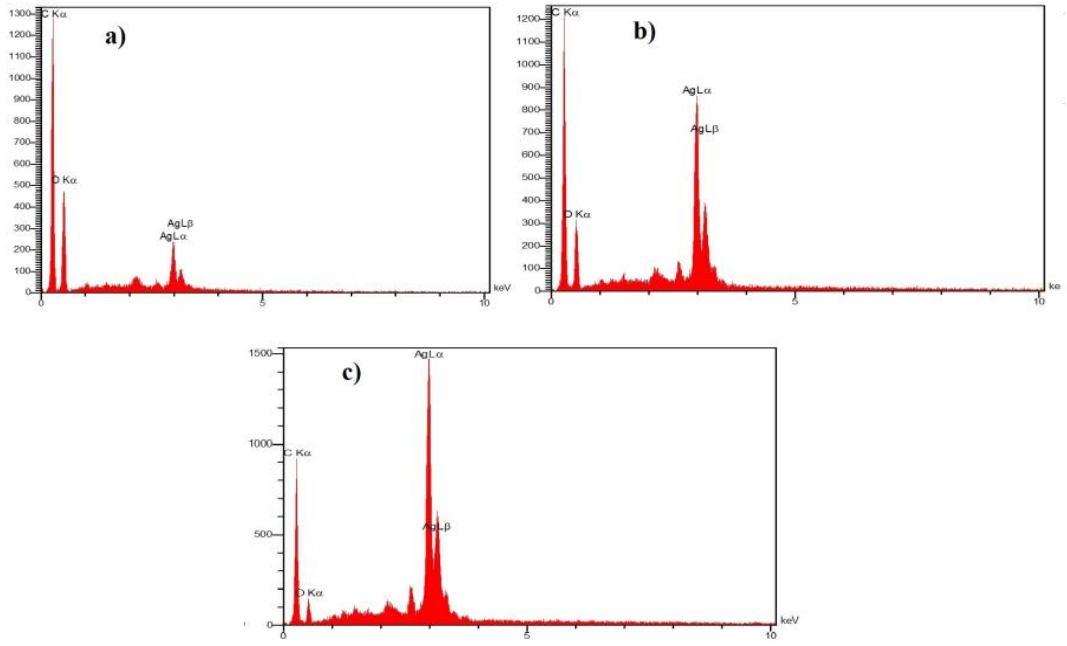

Fig. 9. EDS analysis of XSBL-pretreated and untreated cotton fabric

Table 4. Elemental analysis of XSBL-pretreated and untreated cotton fabric

Pretreated cotton fabric with XSBL			
Number of printed layers / Element	1	5	10
C	54.16	48.42	39.36
O	37.00	23.22	11.12
Ag	8.84	28.35	49.52

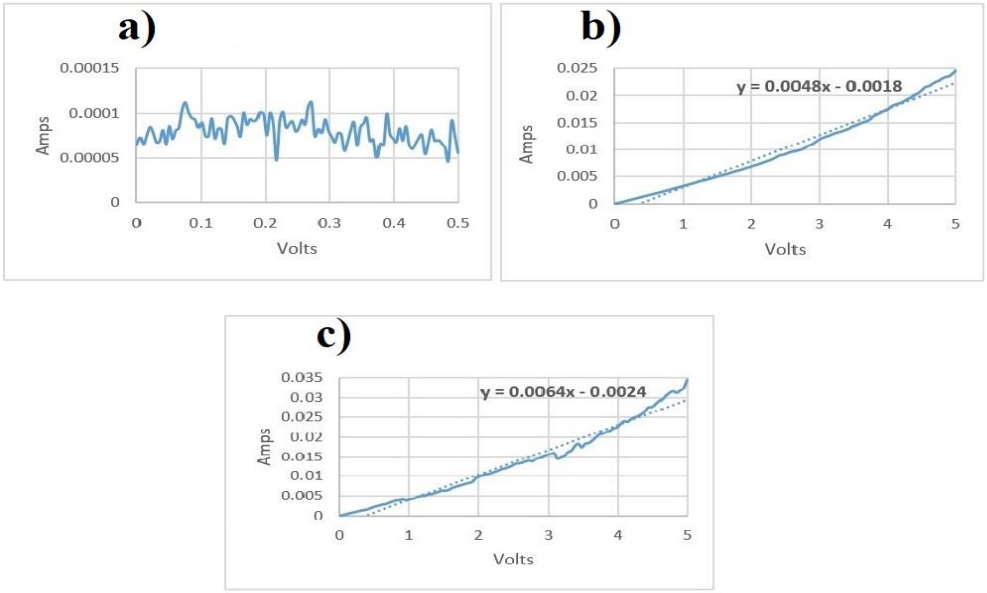

Fig. 10. ampere/voltage diagram of printed samples

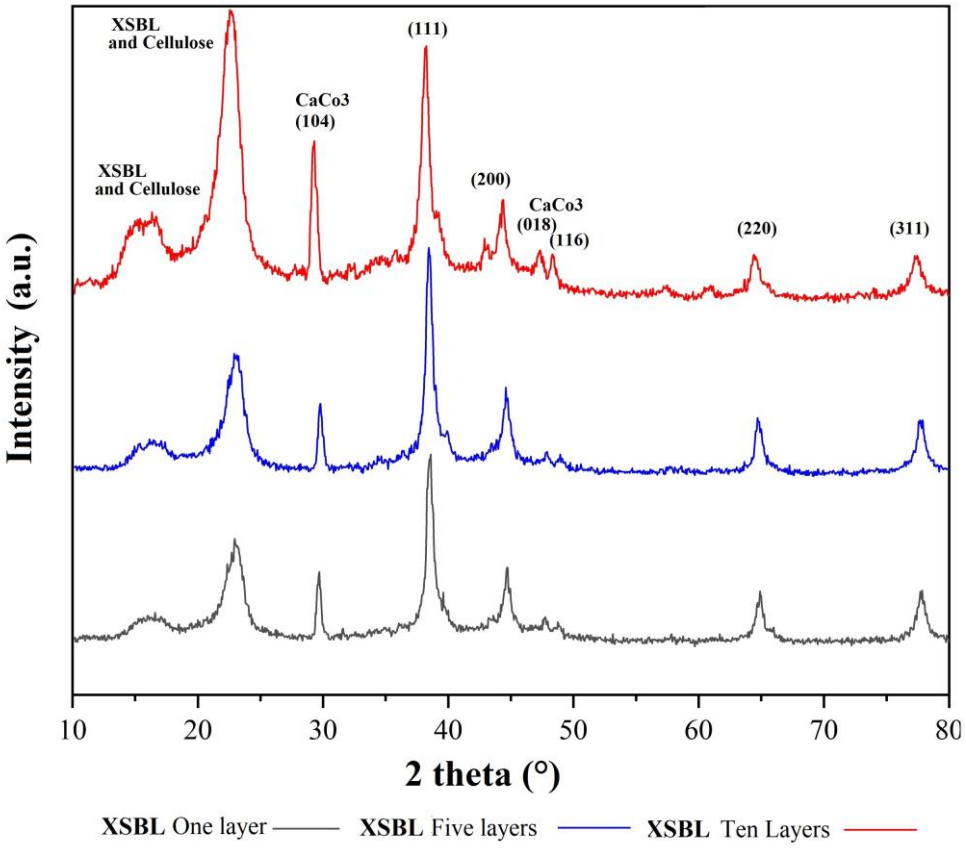

Fig. 11. XRD analysis of inkjet ink printed XSBL-pretreated cotton fabric

Table 5. Resistance/sheet resistance of printed samples

	Number of printed layers	Resistance (Ohm)	Sheet Resistance (Ohm/sq.)
Untreated cotton	1	Out of range	Out of range
	5	Out of range	Out of range
	10	Out of range	Out of range
Pretreated cotton fabric with XSBL	1	Out of range	Out of range
	5	79	335
	10	25	116

Table 6. Resistance/sheet resistance of inkjet ink printed XSBL-pretreated cotton fabric before and after the washing process

Pretreated cotton with XSBL	After washing		Before washing	
Number of printed layers	5	10	5	10
Resistance (Ohm)	95.4	89.46	79	25
Sheet Resistance (Ohm/sq)	404.49	379.3	335	116

XRD analysis of printed layers

XRD diffractograms of the printed pretreated cotton fabric at different printing runs (one, five, and ten) are depicted in Fig. 11. Various Bragg diffractions were detected at 38.2°, 44.3°, 64.5°, and 77.4°. The d- spacing was calculated using the angles extracted from diffraction patterns and the Bragg equation. Considering the atomic radius of silver (1.44 angstrom) and the parameter of the fcc network, the indices of the initial diffraction planes for the fcc structure (h,k,l) was obtained using equation 5 to 7. Where d, r, , and are the space between planes, the atomic radius of silver, the wavelength of CuKα radiation (λ=0.15406 nm) and diffraction angle, respectively. The specified peaks related to the crystallographic planes were ascribed to the faces and miller indices of (111), (200), (220), and (311) respectively (reference card (ICDD 00-004-0783) [50, 51].

$$n\lambda = 2d.sin\theta \quad (5)$$

$$a_{fcc} = 2r\sqrt{2} = \frac{4r}{\sqrt{2}} \quad (6)$$

$$d_{hkl} = \frac{a}{\sqrt{h^2 + l^2 + k^2}} \quad (7)$$

Two broad peaks at 17° and 23° were related to the cellulose structure of the fabric and Miller's indices of (1-10), (110), and (200) [52]. Peaks at 29.5°, 47.8°, and 48.6° (Reference card ICDD 00-047-1743) belonged to calcium carbonate, used as filler and opacifier in XSBL resin [53, 54].

Wash fastness of printed layers

Wash fastness properties of conductive printed layers have been investigated by AATCC 61-2001 standard, with the help of a nonionic emulsifier at 60 ˚C temperature.

As shown in (Table 6), after the washing process, resistivity increased due to detachments of silver nanoparticles on the surface, which were prone

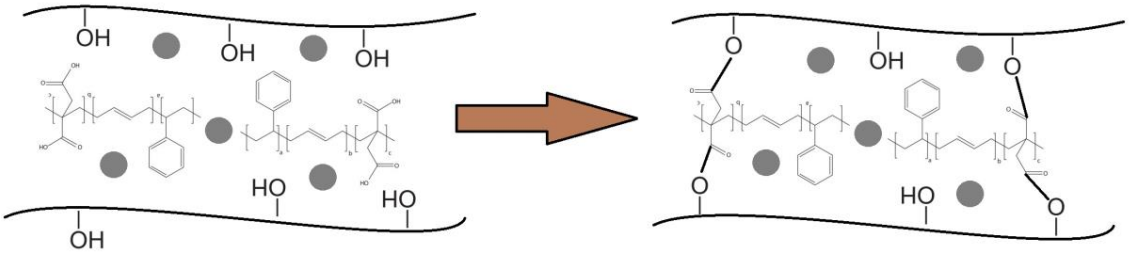

Fig. 12. Cross-link network between cellulose and XSBL to improve wash fastness

Table 7. Inhibition zone of one and five-layer printed samples

	Untreated cotton fabric		Pretreated cotton fabric with XSB	
Number of printed layers	1	5	1	5
Inhabitation (mm) (48 hr.) [Staphylococcus aureus (Gram-positive, ATCC 6538)]	11	12	12	12
Inhabitation (mm) (48 hr.) [Escherichia coli (Gram-negative, ATCC 25922)]	12	12	11	11

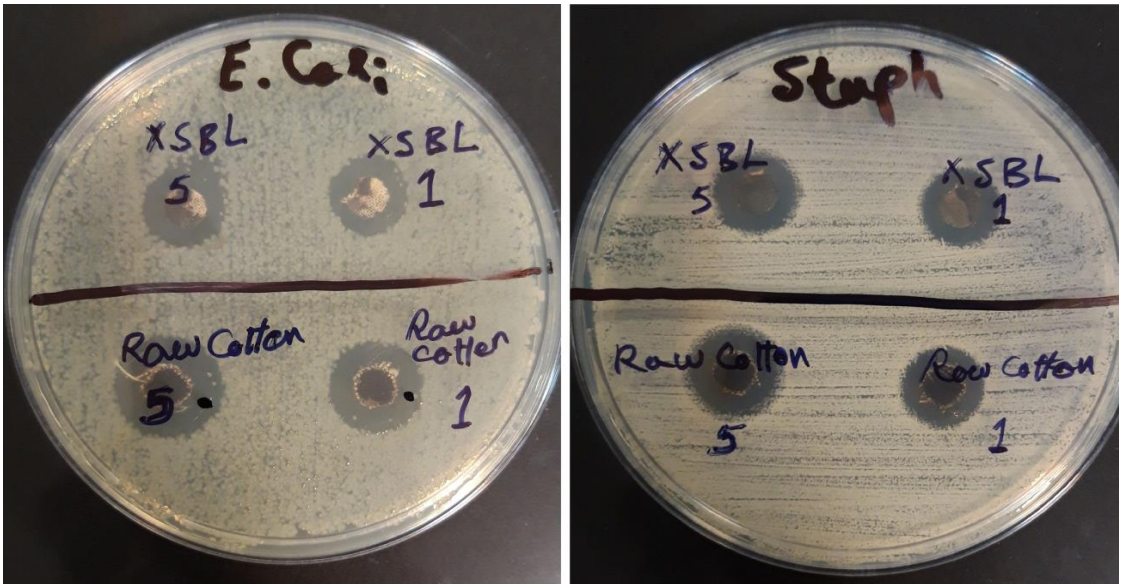

Fig. 13. Image of disc diffusing for one and five layers printed samples

to wash. As a free carboxylic group of XSBL resin can react with the hydroxyl group of cellulose and create a cross-linked network (Fig. 12), silver nanoparticles trapped in the network and wash fastness also improved.

Antimicrobial properties of printed layers

The investigation of the antibacterial property of printed samples, antimicrobial analysis was carried out using the disc diffusion method. The antimicrobial activity is due to the presence and concentration of silver nanoparticles, and to check this property of printed samples, one and five layers of printed fabrics have been selected with lower silver nanoparticles concentration. The untreated and XSBL-pretreated cotton fabric's inhibition zone was determined considering the conditions tabulated in (Table 7).

According to the results obtained from FE-SEM and EDS analysis proving the existence of silver nanoparticles on the fabric surface, the one layer and five layers printed XSBL-pretreated cotton fabrics showed an inhibition zone against gram-positive and gram-negative bacteria. There was also an antimicrobial activity for one/five layers of untreated cotton fabric and one layer of XSBL-pretreated cotton fabric, which indicated that silver nanoparticles were also formed on these samples. However, they were not homogenous enough to create a conductive pattern but enough to have antimicrobial activity. Silver nanoparticles antimicrobial activity have been considered widely. In terms of antimicrobial mechanism, silver nanoparticles mainly kill microorganisms by ion release and cell membrane damage, DNA interaction and reactive oxygen species (ROS) [55]. Gram-negative and gram-positive bacteria's differential sensitivity toward silver nanoparticles

is probably due to their cell wall structure distinction. The cell walls of gram-negative bacteria are comprised of a thin layer of peptidoglycan; however, gram-positive bacteria comprising linear polysaccharide chains cross-linked by short peptides, creating a more rigid structure that is challenging for silver nanoparticles to penetrate [56]. Regarding E. coli bacteria, silver nanoparticles prevent bacteria spread by destroying the permeability of the bacterial membranes [57]. Staphylococcus aureus bacteria exposure to silver nanoparticles causes cell content release in the environment [58].

CONCLUSION

The cotton fabric's porosity and high surface roughness avoid electrically conductive printed patterns on the cotton fabrics. For this purpose, cotton fabric was pretreated with carboxylated styrene-butadiene latex (XSBL). The pretreating process did not have an adverse effect on thermal behavior and colorimetric properties and provided a fabric with soft hand touching and a good wrinkle recovery angle. A water-based silver free-particles ink was prepared with a facile method to print on pretreated cotton fabric via a single-stage inkjet printer to create multi-purpose fabric. After the printing process, silver nanoparticles were formed on the fabric's surface, which improved the electrical conductivity (25 ohm), antibacterial activity, and washing fastness properties due to the cross-linked structure between XSBL and cotton. FE-SEM and EDS analysis indicated that the presence of silver nanoparticles increased by increasing the number of printing runs. XRD analysis illustrated the crystal structure of silver nanoparticles. The obtained results confirm that the flexible electronic printed fabric can be used as a multifunctional electronic textile with great potential for commercial mass production.

CONFLICT OF INTEREST

The authors declare that there is no conflict of interests regarding the publication of this manuscript.

REFERENCES

1. Ko SH, Chung J, Pan H, Grigoropoulos CP, Poulikakos D. Fabrication of multilayer passive and active electric components on polymer using inkjet printing and low temperature laser processing. Sensors and Actuators A: Physical. 2007;134(1):161-168.
2. Aleeva Y, Pignataro B. Recent advances in upscalable wet methods and ink formulations for printed electronics. Journal of Materials Chemistry C. 2014;2(32):6436-6453.
3. De Gans BJ, Duineveld PC, Schubert US. Inkjet printing of polymers: state of the art and future developments. Adv Mater. 2004;16(3):203-213.
4. Chen S, Pua S, Zhong Z, Shan X. Investigation of Roll-to-Roll Gravure Printing for Printed Electronics with Fine Features. Journal of Materials and Applications. 2020;9(2):79-89.
5. Jo M, Lee J, Kim S, Cho G, Lee T-M, Lee C. Resistance Control of an Additively Manufactured Conductive Layer in Roll-to-Roll Gravure Printing Systems. International Journal of Precision Engineering and Manufacturing-Green Technology. 2021;8(3):817-828.
6. Gajadhur M, Regulska M. Mechanical and light resistance of flexographic conductive ink films intended for printed electronics. Dyes and Pigments. 2020;178:108381.
7. Zhong Z, Ee J, Chen S, Shan X. Parametric investigation of flexographic printing processes for R2R printed electronics. Mater Manuf Processes. 2020;35(5):564-571.
8. Hong H, Jiyong H, Moon K-S, Yan X, Wong C-p. Rheological properties and screen printability of UV curable conductive ink for flexible and washable E-textiles. Journal of Materials Science & Technology. 2021;67:145-155.
9. Liu L, Shen Z, Zhang X, Ma H. Highly conductive graphene/carbon black screen printing inks for flexible electronics. Journal of Colloid and Interface Science. 2021;582:12-21.
10. Krebs FC. Fabrication and processing of polymer solar cells: A review of printing and coating techniques. Sol Energy Mater Sol Cells. 2009;93(4):394-412.
11. Ummartyotin S, Juntaro J, Wu C, Sain M, Manuspiya H. Deposition of PEDOT: PSS nanoparticles as a conductive microlayer anode in OLEDs device by desktop inkjet printer. Journal of Nanomaterials. 2011;2011.
12. Hengge M, Livanov K, Zamoshchik N, Hermerschmidt F, List-Kratochvil EJ. ITO-free OLEDs utilizing inkjet-printed and low temperature plasma-sintered Ag electrodes. Flexible and Printed Electronics. 2021;6(1):015009.
13. Liew Q, Rashid NA, Lee H, Hawari H, Khir MM, editors. Inkjet-Printed Flexible Temperature Sensor using Hybrid Reduced Graphene Oxide–Silver Nanoparticles (rGO/AgNPs) Conductive Ink and Silver Nanoparticles Ink. Journal of Physics: Conference Series; 2021: IOP Publishing.
14. Bidoki S, Lewis D, Clark M, Vakorov A, Millner P, McGorman D. Ink-jet fabrication of electronic components. Journal of Micromechanics and Microengineering. 2007;17(5):967.
15. Jung M, Kim J, Noh J, Lim N, Lim C, Lee G, et al. All-printed and roll-to-roll-printable 13.56-MHz-operated 1-bit RF tag on plastic foils. IEEE Trans Electron Devices. 2010;57(3):571-580.
16. Fathi P, Shrestha S, Yerramilli R, Karmakar N, Bhattacharya S. Screen printed chipless RFID tags on packaging substrates. Flexible and Printed Electronics. 2021;6(2):025009.
17. Htwe Y, Mariatti M. Surfactant-assisted water-based graphene conductive inks for flexible electronic applications. Journal of the Taiwan Institute of Chemical Engineers. 2021.
18. Fernandes IJ, Aroche AF, Schuck A, Lamberty P, Peter CR, Hasenkamp W, et al. Silver nanoparticle conductive inks: Synthesis, characterization, and fabrication of inkjet-printed flexible electrodes. Sci Rep. 2020;10(1):1-11.
19. Truong T, Kim J-S, Kim J. Design and Optimization of Embroidered Antennas on Textile Using Silver Conductive Thread for Wearable Applications. Fibers and Polymers. 2021:1-10.

20. Akindoyo JO, Ismail NH, Mariatti M. Development of environmentally friendly inkjet printable carbon nanotube-based conductive ink for flexible sensors: effects of concentration and functionalization. Journal of Materials Science: Materials in Electronics. 2021;32(9):12648-12660.
21. Barani H, Miri A, Sheibani H. Comparative study of electrically conductive cotton fabric prepared through the in situ synthesis of different conductive materials. Cellulose. 2021:1-21.
22. Trovato V, Teblum E, Kostikov Y, Pedrana A, Re V, Nessim GD, et al. Electrically conductive cotton fabric coatings developed by silica sol-gel precursors doped with surfactant-aided dispersion of vertically aligned carbon nanotubes fillers in organic solvent-free aqueous solution. Journal of Colloid and Interface Science. 2021;586:120-134.
23. Kang Z, He Y, Sang J, Hirahara H, Chen D. Superhydrophobic and Conductive Cotton Fabric Composite with Excellent Corrosion Resistance for Wearable Electronics. Advanced Materials Interfaces. 2021:2100651.
24. Liu S, Hu M, Yang J. A facile way of fabricating a flexible and conductive cotton fabric. Journal of Materials Chemistry C. 2016;4(6):1320-1325.
25. Singh J, Singh N, Rathi A, Kukkar D, Rawat M. Facile approach to synthesize and characterization of silver nanoparticles by using mulberry leaves extract in aqueous medium and its application in antimicrobial activity. 2017.
26. Thomas B, Arul Prasad A, Mary Vithiya S. Evaluation Of Antioxidant, Antibacterial And Photo Catalytic Effect Of Silver Nanoparticles From Methanolic Extract Of Coleus Vettiveroids–An Endemic Species. Journal of Nanostructures. 2018;8(2):179-190.
27. Tolouietabar H, Hatamnia AA, Sahraei R, Soheyli E. Biologically Green Synthesis of High-quality Silver Nanoparticles Using Scrophularia striata Boiss Plant Extract and Verifying Their Antibacterial Activities. Journal of Nanostructures. 2020;10(1):44-51.
28. Chou K-S, Ren C-Y. Synthesis of nanosized silver particles by chemical reduction method. Materials chemistry and physics. 2000;64(3):241-246.
29. Montazer M, Nia ZK. Conductive nylon fabric through in situ synthesis of nano-silver: Preparation and characterization. Materials Science and Engineering: C. 2015;56:341-347.
30. Vaseem M, McKerricher G, Shamim A. Robust design of a particle-free silver-organo-complex ink with high conductivity and inkjet stability for flexible electronics. ACS applied materials & interfaces. 2016;8(1):177-186.
31. Li J, Zhang X, Liu X, Liang Q, Liao G, Tang Z, et al. Conductivity and foldability enhancement of Ag patterns formed by PVAc modified Ag complex inks with low-temperature and rapid sintering. Materials & Design. 2020;185:108255.
32. Nie X, Wang H, Zou J. Inkjet printing of silver citrate conductive ink on PET substrate. Appl Surf Sci. 2012;261:554-560.
33. Xu W, Wang T. Synergetic effect of blended alkylamines for copper complex ink to form conductive copper films. Langmuir. 2017;33(1):82-90.
34. Menachem L, Pearce E. Handbook of fiber chemistry. CRC, USA. 2006.
35. Wakelyn PJ, Bertoniere NR, French AD, Thibodeaux DP, Triplett BA, Rousselle M-A, et al. Cotton fiber chemistry and technology: CRC Press; 2006.
36. Charmot D, D'Allest J, Dobler F. Carboxylated styrene-butyl acrylate and styrene-butadiene emulsion copolymers. Modelling the distribution of the acid monomer between serum, particle surface and the particle core. Polymer. 1996;37(23):5237-5245.
37. Stephen R, Siddique A, Singh F, Kailas L, Jose S, Joseph K, et al. Thermal degradation and ageing behavior of microcomposites of natural rubber, carboxylated styrene butadiene rubber latices, and their blends. J Appl Polym Sci. 2007;105(2):341-351.
38. Berki P, Göbl R, Karger-Kocsis J. Structure and properties of styrene-butadiene rubber (SBR) with pyrolytic and industrial carbon black. Polym Test. 2017;61:404-415.
39. Mukhopadhyay S, Sahu P, Bhajiwala H, Mohanty S, Gupta V, Bhowmick AK. Synthesis, characterization and properties of self-healable ionomeric carboxylated styrene–butadiene polymer. Journal of Materials Science. 2019;54(24):14986-14999.
40. Babu KF, Senthilkumar R, Noel M, Kulandainathan MA. Polypyrrole microstructure deposited by chemical and electrochemical methods on cotton fabrics. Synth Met. 2009;159(13):1353-1358.
41. Nair MR, Thomas GV, Nair MG. Thermogravimetric analysis of PVC/ELNR blends. Polymer Degradation and Stability. 2007;92(2):189-196.
42. Aminayi P, Abidi N. Ultra-oleophobic cotton fabric prepared using molecular and nanoparticle vapor deposition methods. Surf Coat Technol. 2015;276:636-644.
43. Le C, Ly N, Stevens M. Measuring the contact angles of liquid droplets on wool fibers and determining surface energy components. Textile Research Journal. 1996;66(6):389-397.
44. Peršin Z, Stenius P, Stana-Kleinschek K. Estimation of the surface energy of chemically and oxygen plasma-treated regenerated cellulosic fabrics using various calculation models. Textile research journal. 2011;81(16):1673-1685.
45. Wang C-C, Chen C-C. Physical properties of the crosslinked cellulose catalyzed with nanotitanium dioxide under UV irradiation and electronic field. Applied Catalysis A: General. 2005;293:171-179.
46. Reyes-Labarta J, Herrero M, Tiemblo P, Mijangos C, Reinecke H. Wetchemical surface modification of plasticized PVC. Characterization by FTIR-ATR and Raman microscopy. Polymer. 2003;44(8):2263-2269.
47. Riaz S, Ashraf M, Hussain T, Hussain MT, Younus A. Fabrication of Robust Multifaceted Textiles by Application of Functionalized TiO_2 Nanoparticles. Colloids Surf Physicochem Eng Aspects. 2019;581:123799.
48. Dima S-O, Panaitescu D-M, Orban C, Ghiurea M, Doncea S-M, Fierascu RC, et al. Bacterial nanocellulose from side-streams of Kombucha beverages production: Preparation and physical-chemical properties. Polymers. 2017;9(8):374.
49. Ma L, Liu M, Peng Q, Liu Y, Luo B, Zhou C. Crosslinked carboxylated SBR composites reinforced with chitin nanocrystals. Journal of Polymer Research. 2016;23(7):134.
50. Cai Y, Piao X, Gao W, Zhang Z, Nie E, Sun Z. Large-scale and facile synthesis of silver nanoparticles via a microwave method for a conductive pen. RSC advances. 2017;7(54):34041-34048.
51. Zhang H, Zhang C. Transport of silver nanoparticles capped with different stabilizers in water saturated porous media. Journal of Materials and Environmental Science. 2014;5(1):231-236.
52. French AD. Idealized powder diffraction patterns for cellulose polymorphs. Cellulose. 2014;21(2):885-896.
53. Luo X, Song X, Cao Y, Song L, Bu X. Investigation of calcium

carbonate synthesized by steamed ammonia liquid waste without use of additives. RSC Advances. 2020;10(13):7976-7986.
54. Wei H, Shen Q, Zhao Y, Wang D, Xu D. Crystallization habit of calcium carbonate in presence of sodium dodecyl sulfate and/or polypyrrolidone. J Cryst Growth. 2004;260(3-4):545-550.
55. Durán N, Durán M, De Jesus MB, Seabra AB, Fávaro WJ, Nakazato G. Silver nanoparticles: A new view on mechanistic aspects on antimicrobial activity. Nanomed Nanotechnol Biol Med. 2016;12(3):789-799.
56. Franci G, Falanga A, Galdiero S, Palomba L, Rai M, Morelli G, et al. Silver nanoparticles as potential antibacterial agents. Molecules. 2015;20(5):8856-8874.
57. Li W-R, Xie X-B, Shi Q-S, Zeng H-Y, You-Sheng O-Y, Chen Y-B. Antibacterial activity and mechanism of silver nanoparticles on Escherichia coli. Applied microbiology and biotechnology. 2010;85(4):1115-1122.
58. Li W-R, Xie X-B, Shi Q-S, Duan S-S, Ouyang Y-S, Chen Y-B. Antibacterial effect of silver nanoparticles on Staphylococcus aureus. BioMetals. 2011;24(1):135-141.